

Supporting Information

Nondoped blue fluorescent organic light-emitting diodes based on benzonitrile-anthracene derivative with 10.06 % external quantum efficiency and low efficiency roll-off

Wei Liu,^a Shian Ying,^b Runda Guo,^a Xianfeng Qiao,^b Panpan Leng,^a Qing Zhang,^a Yaxiong Wang,^a Dongge Ma^{*b} and Lei Wang^{*a}

^a Wuhan National Laboratory for Optoelectronics, Huazhong University of Science and Technology, Wuhan, 430074, People's Republic of China.

^b Institute of Polymer Optoelectronic Materials and Devices, State Key Laboratory of Luminescent Materials and Devices, South China University of Technology, Guangzhou 510640, People's Republic of China.

*Email: msdgma@scut.edu.cn, wanglei@mail.hust.edu.cn

Content

1. Solvatochromic effect.
2. Fig. S1. Thermogravimetric analysis (TGA) and Differential scanning calorimetry (DSC) curves.
3. Table S1. Nondoped electroluminescent performances for some representative blue-emitting materials.
4. Table S2. The absorption and emission peak positions in different solvents.
5. Fig. S2. The absorption (UV) spectra of AnBzt in dichloromethane.
6. Fig. S3. Schematic molecular conformations and interactions of 3CzAnBzt in the crystal.
7. Fig. S4. Schematic molecular conformations and interactions of *p*CzAnBzt in the crystal.
8. Fig. S5. The PL spectra of 3CzAnBzt and *p*CzAnBzt in different solvents.
9. Fig. S6. Fitted line of Δf and $v_a - v_f$ for 3CzAnBzt and *p*CzAnBzt.
10. Table S3. Crystal data.
11. Fig. S7. Cyclic voltammetric scans.
12. Fig. S8. NTOs of 3CzAnBzt.
13. Fig. S9. NTOs of *p*CzAnBzt.
14. Fig. S10. Energy diagram of 3CzAnBzt and *p*CzAnBzt.
15. Fig. S11. The EL spectrum with different applied bias of 3CzAnBzt and *p*CzAnBzt.
16. Fig. S12. J-V characteristics of hole-only and electron-only of 3CzAnBzt and *p*CzAnBzt.

17. Fig. S13. EQE as a function of brightness of doped devices for 3CzAnBzt and *p*CzAnBzt.

18. Table S4. The doped EL performances of 3CzAnBzt and *p*CzAnBzt.

1.Solvatochromic effect

Lippert–Mataga equation:

$$hc(\vartheta_a - \vartheta_f) = hc(\vartheta_a^\circ - \vartheta_f^\circ) - \frac{2(\mu_e - \mu_g)^2}{a^3} f(\varepsilon, n) \quad \text{Equation 1}$$

$f(\varepsilon, n)$: the orientational polarizability of solvents.

ε : the solvent dielectric.

n : the solvent refractive index.

μ_e : the excited state dipole moment.

μ_g : the ground state dipole moment.

a : the solvent cavity (Onsager) radius

$$f(\varepsilon, n) = \frac{\varepsilon - 1}{2\varepsilon + 1} - \frac{n^2 - 1}{2n^2 + 1}; a = (3M/4N\pi d)^{1/3} \quad \text{Equation 2}$$

N : avogadro number.

M : molecular weight.

d : density ($d = 1.0 \text{ g cm}^{-3}$).

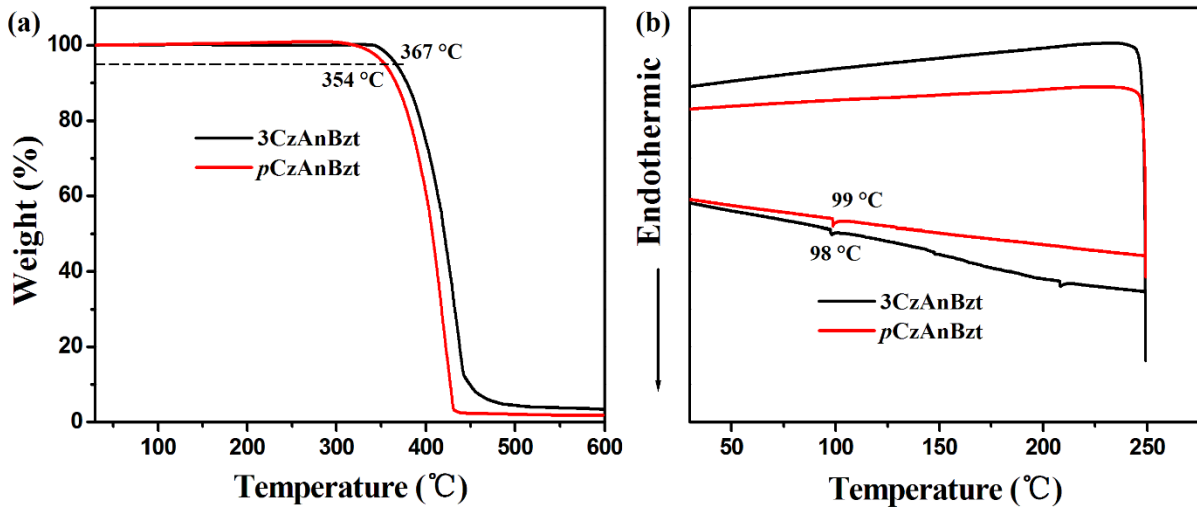


Fig. S1. (a) Thermogravimetric analysis (TGA) and (b) Differential scanning calorimetry (DSC) curves of **3CzAnBzt** and **pCzAnBzt**.

Table S1. Nondoped electroluminescent performances for some representative blue-emitting materials.

| Compound | $\text{CE}_{\text{max}/1000^{\text{a}}}$ (cd A $^{-1}$) | $\text{EQE}_{\text{max}/1000^{\text{a}}}$ (%) | λ_{EL} (nm) | CIE (x, y) | Ref. |
|-------------------|--|---|----------------------------|--------------|-----------|
| 3CzAnBzt | 11.72/10.17 | 10.06/8.97 | 463 | (0.14, 0.14) | This work |
| pCzAnBzt | 8.22/6.07 | 9.23/7.10 | 454 | (0.14, 0.10) | This work |
| PIAnCN | 13.16/- | 9.44/9.44 | 470 | (0.14, 0.19) | 47 |
| DMAC-DPS | - | 19.5/14.6 | 480 | (0.16, 0.29) | 30 |
| Blu2 | 3.34 | 7.40/- | 493 | (0.15, 0.29) | 12 |
| PPI-2TPA | 4.4/- | 7.20/6.30 | 440 | (0.15, 0.06) | 45 |
| TPA-PA | 4.07/- | 7.23/- | 428 | (0.16, 0.07) | 14 |
| TAT | 3.64/- | 7.18/- | 444 | (0.16, 0.09) | 9 |
| N1-1-PhTPA | 6.35/5.70 | 6.08/5.46 | 458 | (0.14, 0.12) | 38 |
| BBTPI | 5.48 | 5.77/5.41 | 448 | (0.15, 0.10) | 15 |
| TPAXAN | - | 4.62/- | 428 | (0.16, 0.05) | 16 |

^a CE and EQE of maximum / at 1000 cd m $^{-2}$.**Table S2.** Detailed information of absorption and emission peak positions of **3CzAnBzt** and **pCzAnBzt** in different solvents at an identical concentration of 10 $^{-5}$ M.

| Solvent | ε | n | Δf | 3CzAnBzt | | | pCzAnBzt | | |
|--------------------|---------------|-------|------------|---------------------|---------------------|------------------------------|---------------------|---------------------|------------------------------|
| | | | | λ_a (nm) | λ_f (nm) | v_{a-v_f} (cm $^{-1}$) | λ_a (nm) | λ_f (nm) | v_{a-v_f} (cm $^{-1}$) |
| <i>n</i> -Hexane | 1.58 | 1.381 | 0.001 | 394 | 434 | 2339.2 | 393 | 426 | 1971.1 |
| Toluene | 2.38 | 1.494 | 0.014 | 398 | 442 | 2501.2 | 396 | 434 | 2211.1 |
| Dioxane | 2.21 | 1.422 | 0.021 | 396 | 442 | 2628.1 | 395 | 433 | 2221.8 |
| Triethylamine | 2.42 | 1.401 | 0.048 | 394 | 438 | 2549.7 | 393 | 428 | 2080.8 |
| Choloroform | 4.81 | 1.443 | 0.149 | 397 | 449 | 2917.2 | 396 | 438 | 2421.5 |
| Ethyl ether | 4.34 | 1.352 | 0.167 | 394 | 446 | 2959.2 | 392 | 436 | 2574.4 |
| Ethyl aceyate | 6.02 | 1.372 | 0.200 | 394 | 446 | 2959.2 | 393 | 433 | 2350.6 |
| Tetrahydrofuran | 7.58 | 1.407 | 0.210 | 397 | 448 | 2867.5 | 395 | 436 | 2380.7 |
| Methylene chloride | 8.93 | 1.424 | 0.217 | 398 | 454 | 3099.2 | 396 | 438 | 2421.5 |

| | | | | | | | | | |
|--------------------|------|-------|-------|-----|-----|--------|-----|-----|--------|
| Dimethyl formamide | 37.0 | 1.427 | 0.276 | 398 | 464 | 3573.9 | 396 | 442 | 2628.1 |
| Acetone | 20.7 | 1.359 | 0.284 | 394 | 452 | 3256.8 | 393 | 437 | 2562.0 |

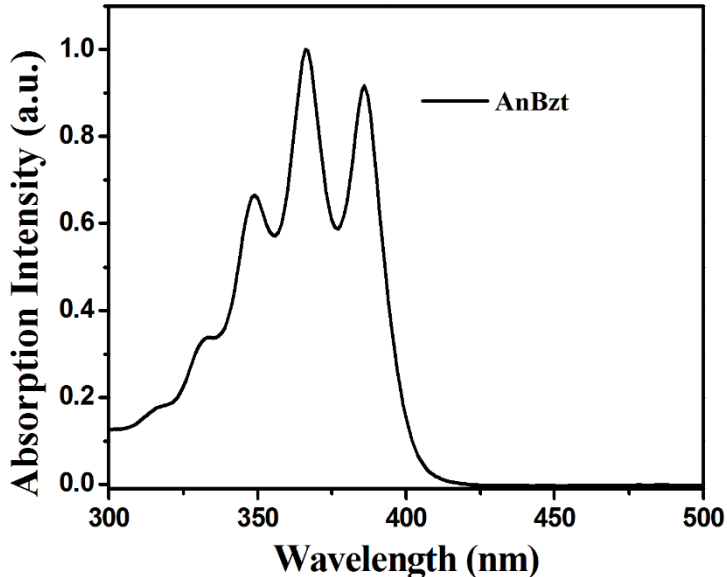


Fig. S2. The absorption (UV) spectra of **AnBzt** in dichloromethane (10^{-5} M).

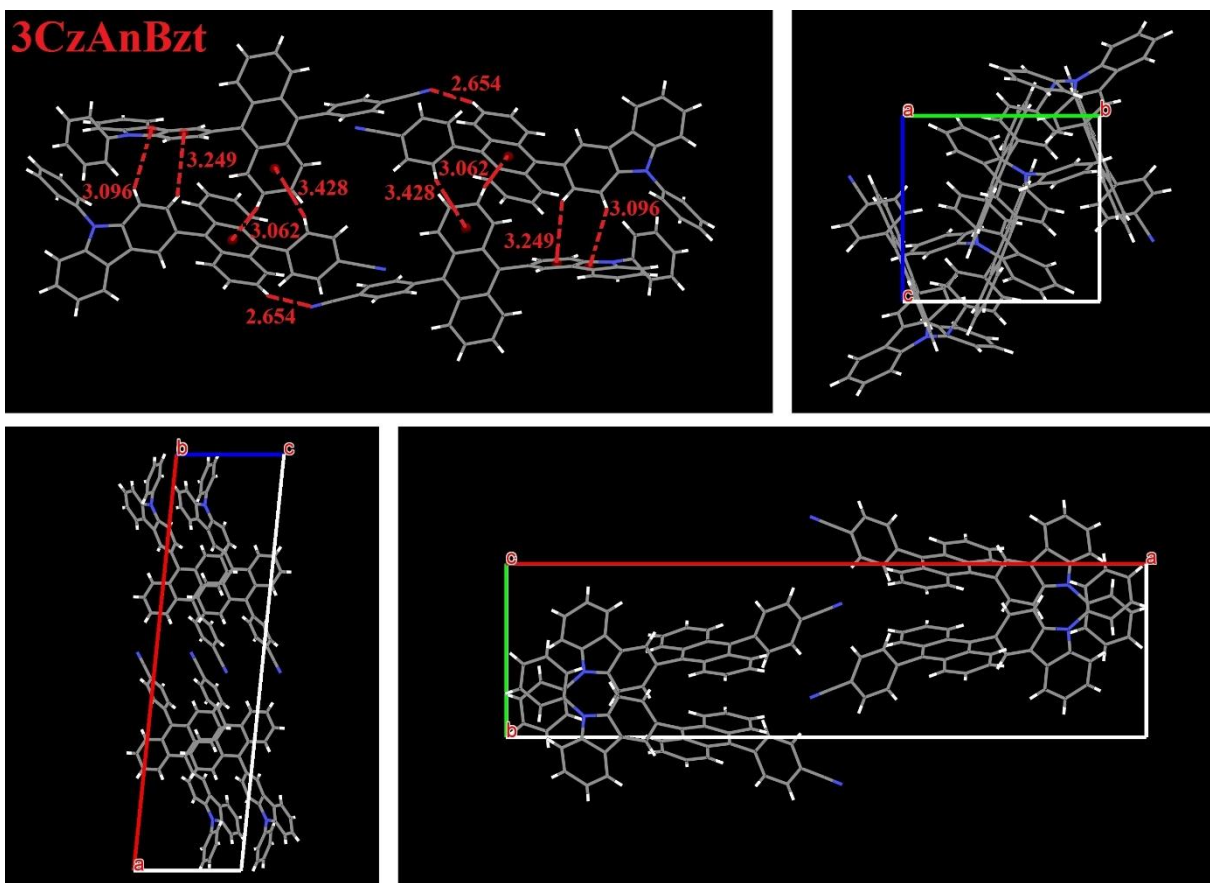


Fig. S3. Schematic molecular conformations and interactions of **3CzAnBzt** in the crystal.

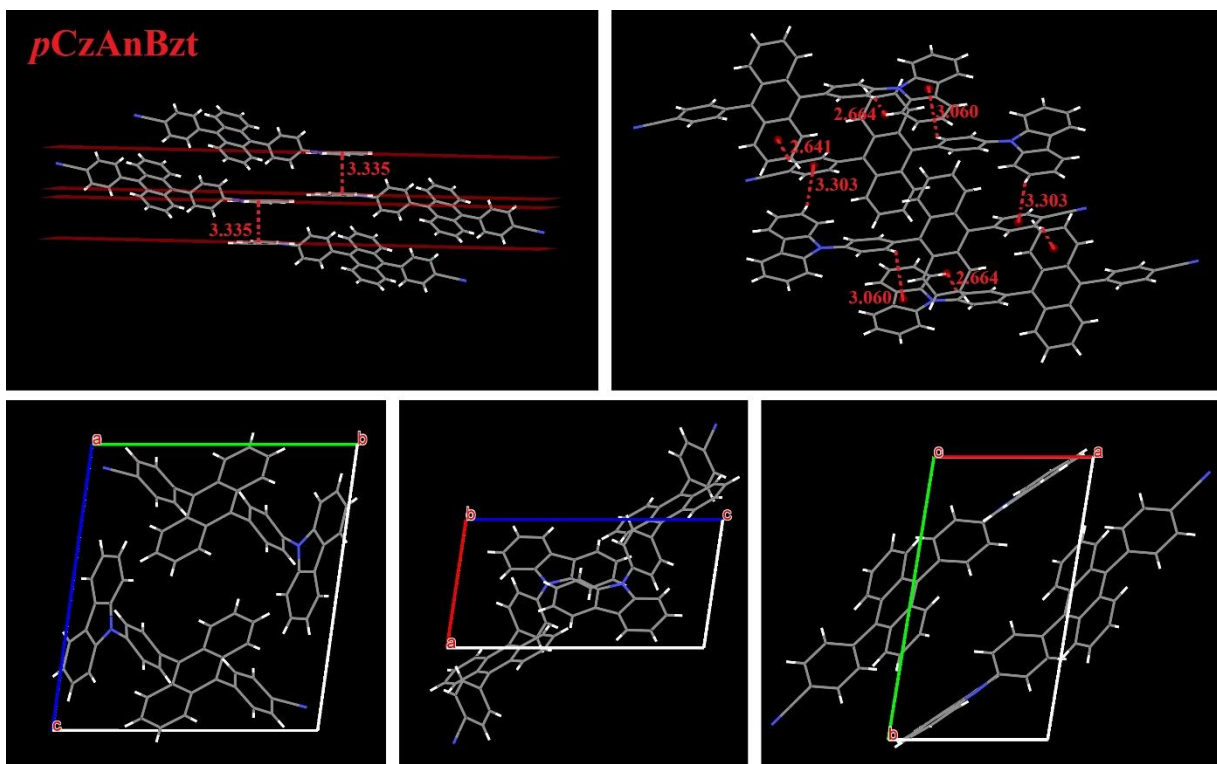


Fig. S4. Schematic molecular conformations and interactions of *p*CzAnBzt in the crystal.

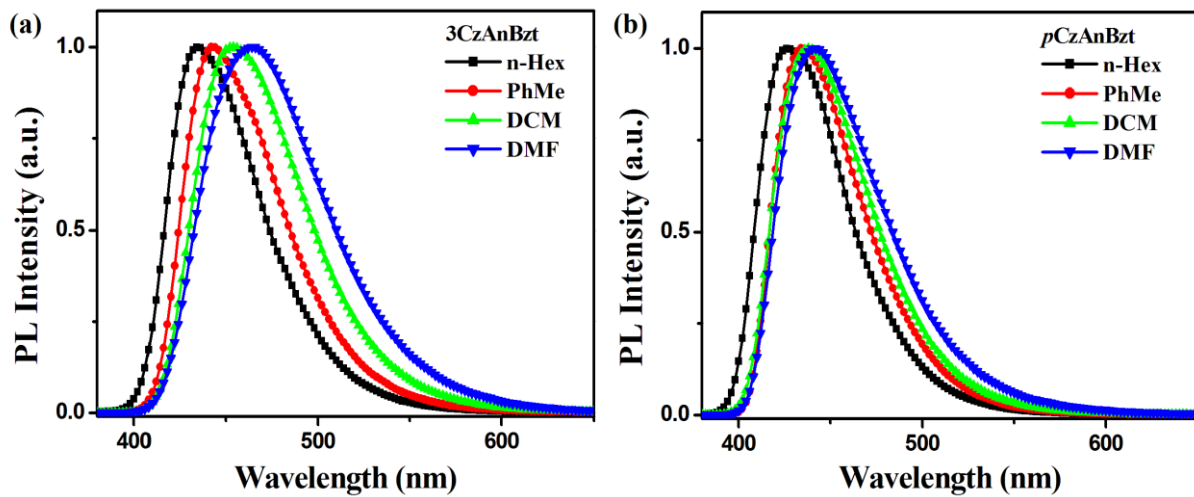


Fig. S5. The emission of **3CzAnBzt** (a) and ***p*CzAnBzt** (b) in different solvents.

Table S3 Crystal data and structure refinement for **3CzAnBzt** and ***p*CzAnBzt**.

| Identification code | 3CzAnBzt | <i>p</i>CzAnBzt |
|-----------------------------|--|--|
| Empirical formula | C ₃₉ H ₂₄ N ₂ | C ₃₉ H ₂₄ N ₂ |
| Formula weight | 520.64 | 520.64 |
| Temperature | 100 K | 100 K |
| Crystal system, space group | Monoclinic, P-1 | Triclinic, P-1 |

| | | |
|--------------------|----------------------------|---------------------------|
| a, Å | 33.7852(9) | 7.4203(2) |
| b, Å | 9.1188(2) | 13.3663(3) |
| c, Å | 8.6590(3) | 14.5908(4) |
| Alpha, deg | 90 | 96.694(2) |
| Beta, deg | 95.866(3) | 97.320(2) |
| Gamma, deg | 90 | 98.178(2) |
| Volume | 2653.70(13) Å ³ | 1407.32(6) Å ³ |
| Calculated density | 1.303 g/cm ³ | 1.229 g/cm ³ |
| F(000) | 1088 | 544 |
| CCDC number | 1857041 | 1857042 |

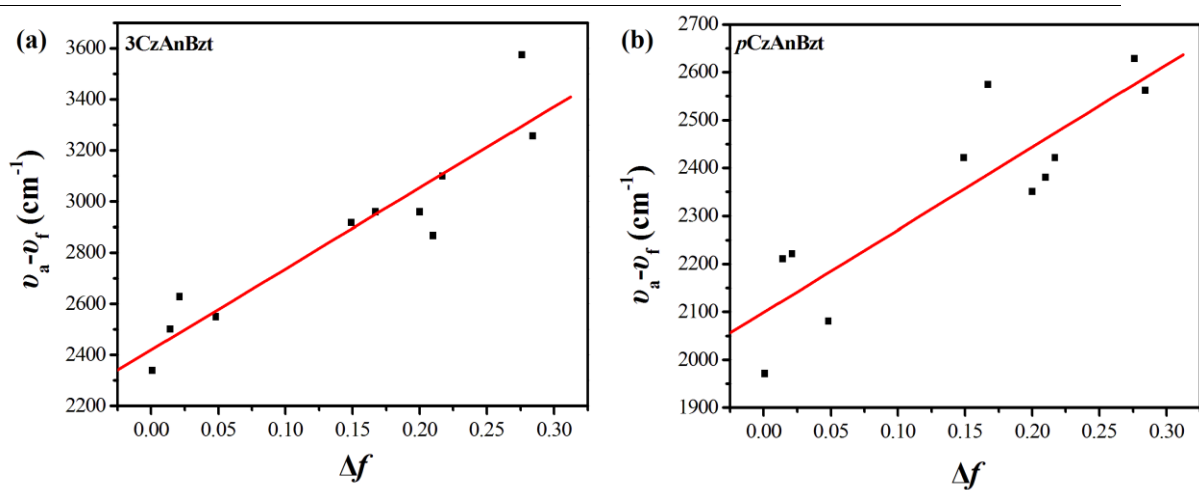


Fig. S6. Linear correlation of orientation polarization (Δf) of solvent media with the Stokes shift ($\nu_a - \nu_f$) for **3CzAnBzt** (a) and **pCzAnBzt** (b).

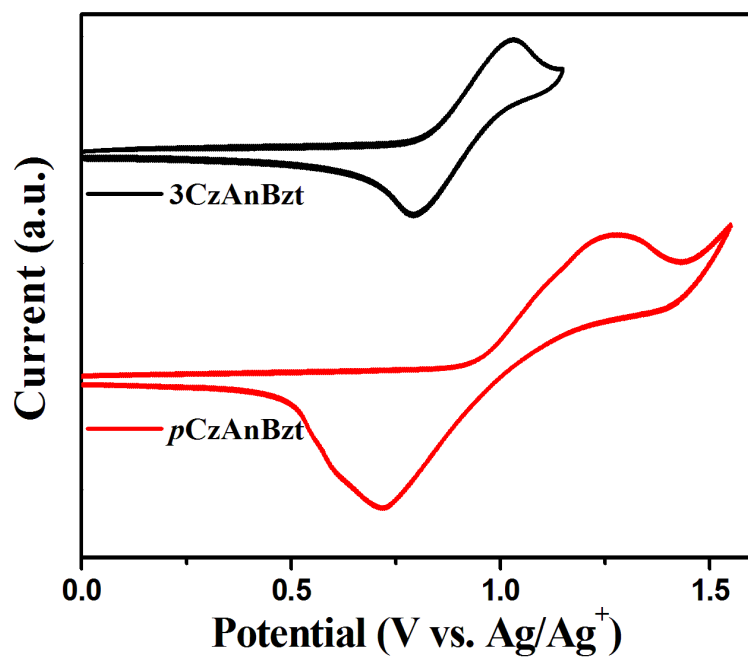


Fig. S7. Cyclic voltammetric scans of **3CzAnBzt** and **pCzAnBzt**.

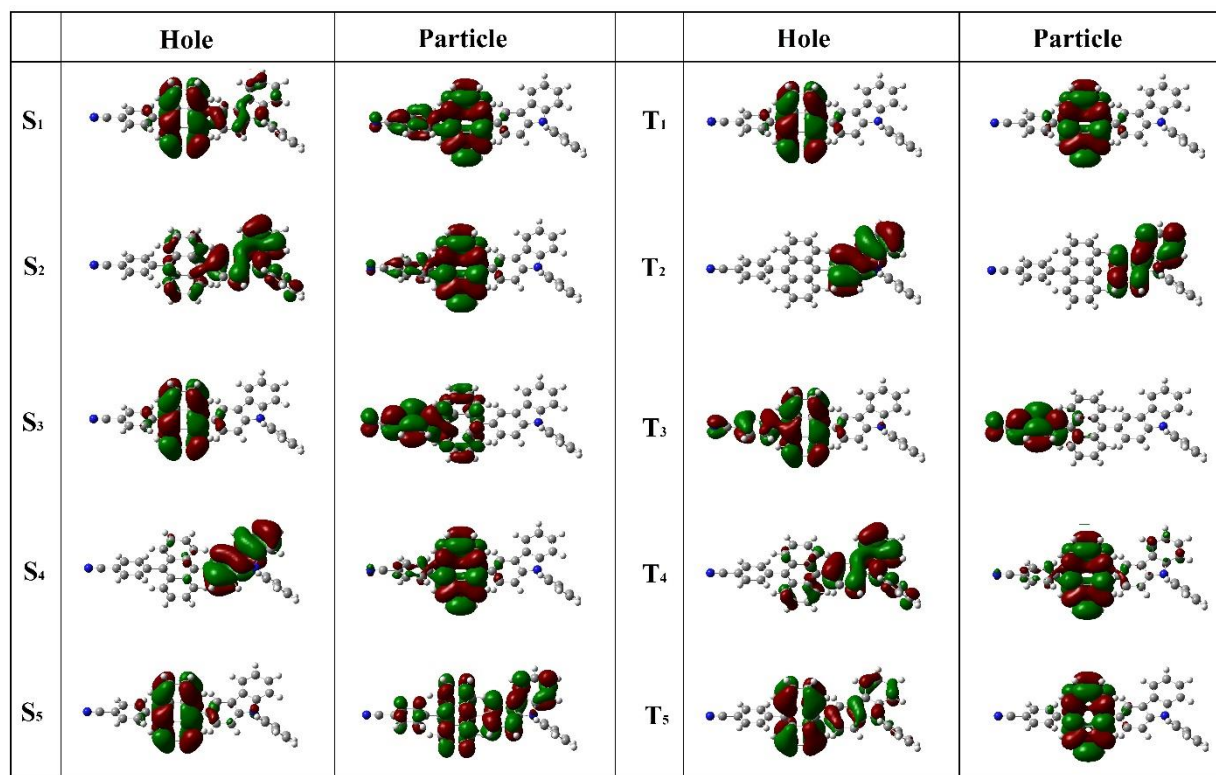


Fig. S8. NTOs of singlet and triplet excited states for **3CzAnBzt**.

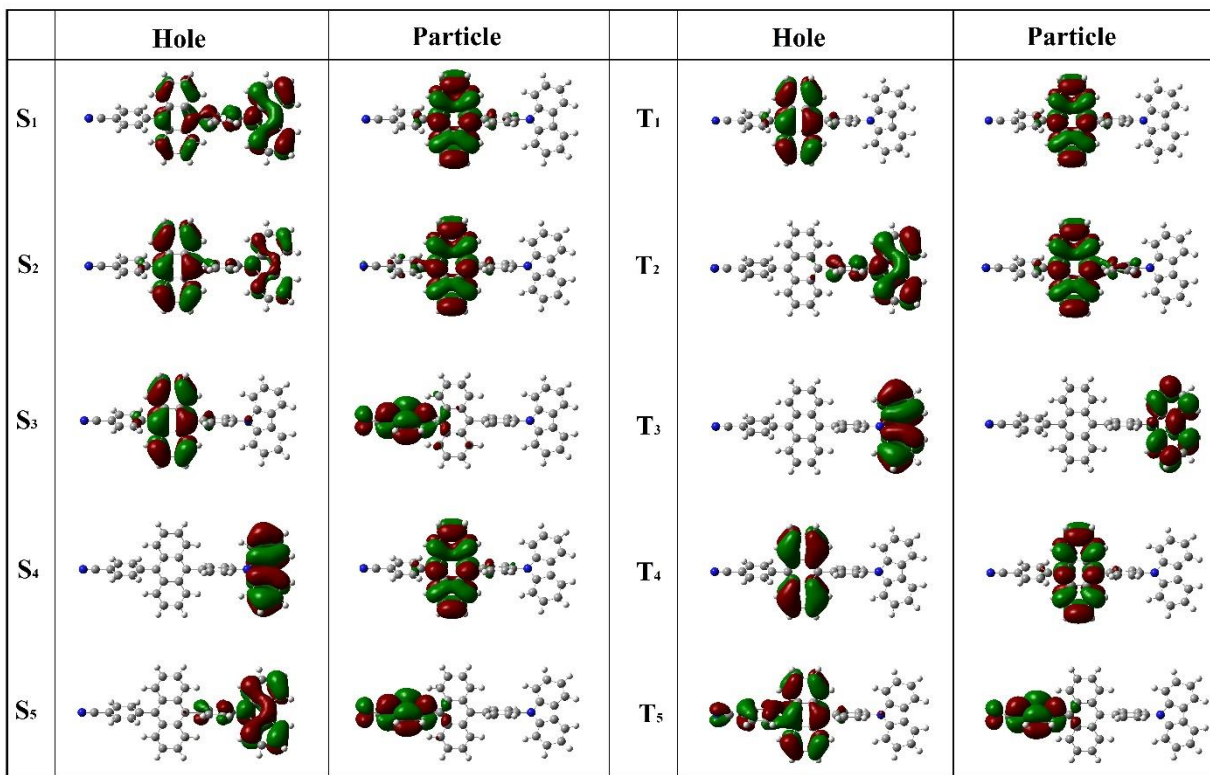


Fig. S9. NTOs of singlet and triplet excited states for *p*CzAnBzt.

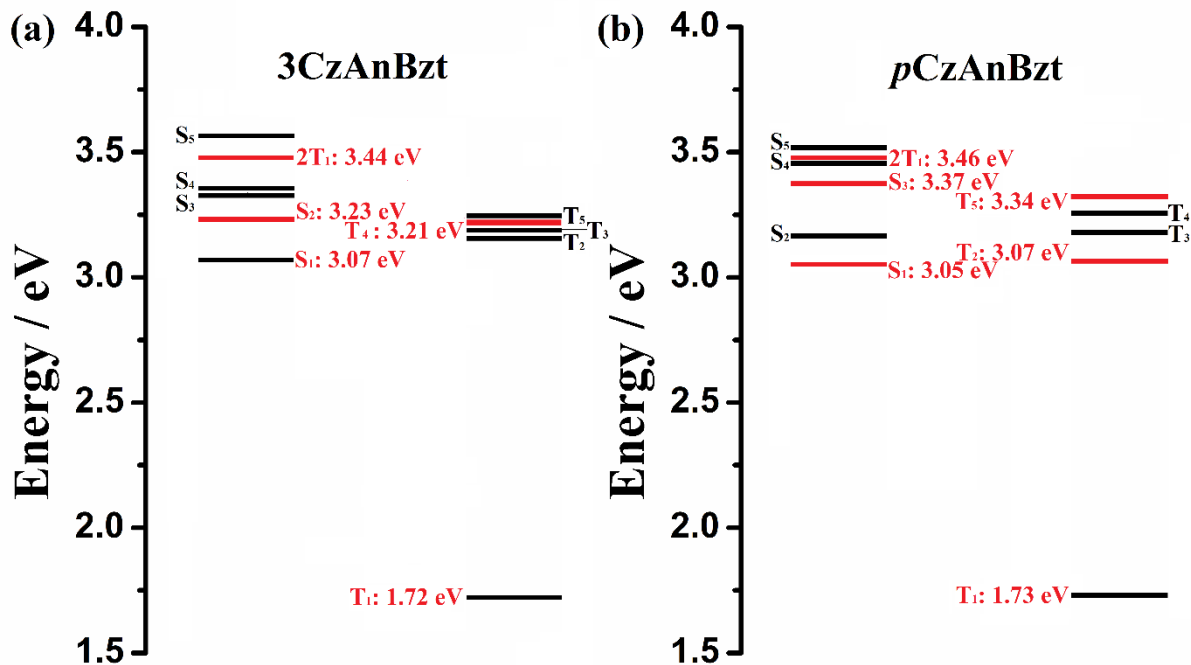


Fig. S10. Energy diagram of calculated singlet and triplet excited states for 3CzAnBzt (a) and *p*CzAnBzt (b).

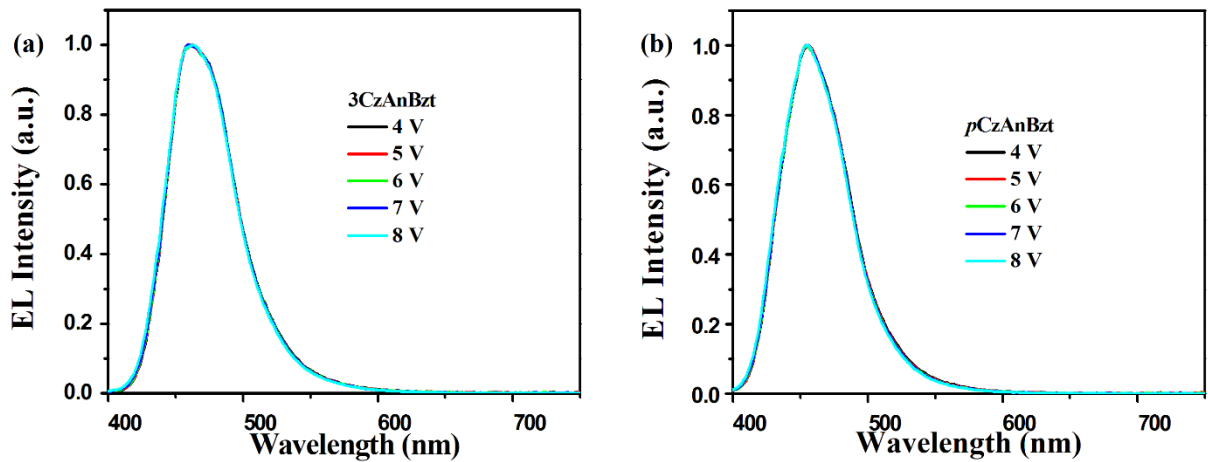


Fig. S11. The EL spectrum with different applied bias of **3CzAnBzt** (a) and **pCzAnBzt** (b).

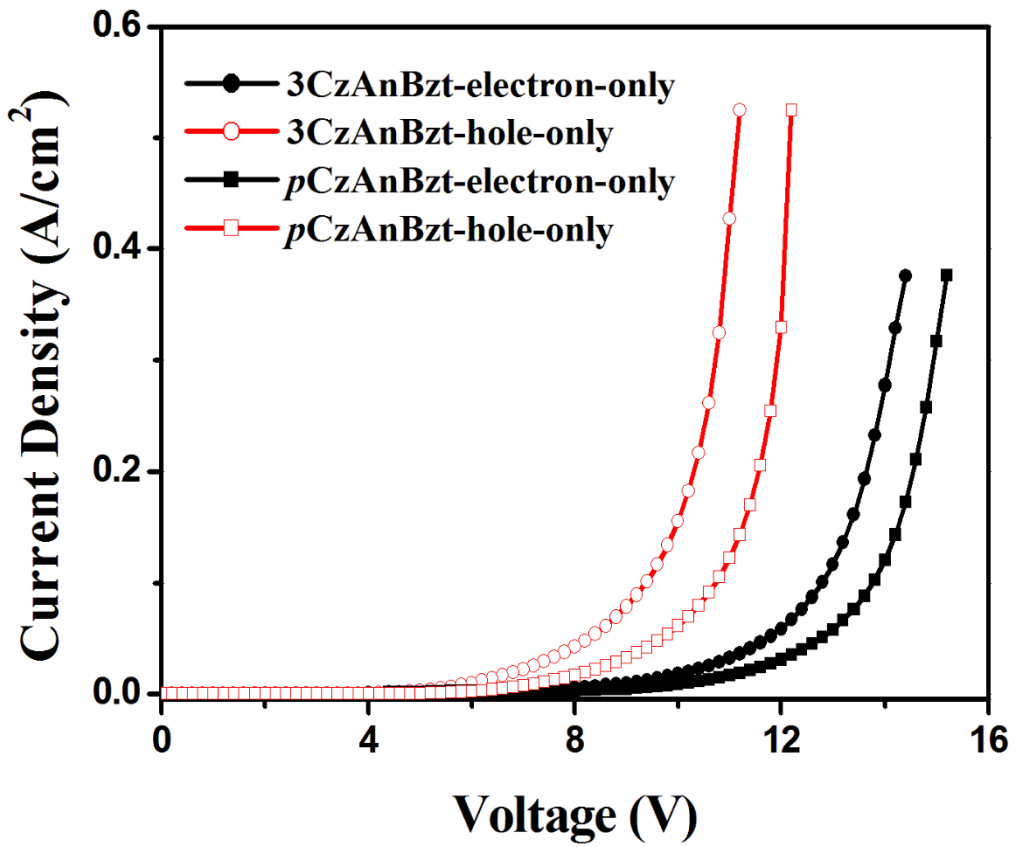


Fig. S12. *J-V* characteristics of hole-only and electron-only of **3CzAnBzt** and **pCzAnBzt**. The devices structure of hole-only: ITO/HATCN (15 nm)/TAPC (50 nm)/TCTA (5 nm)/EML (20 nm)/TCTA (5 nm)/TAPC (50 nm)/HATCN (15 nm)/Al(150 nm), and the devices structure of electron-only: ITO/LiF(1 nm)/TmPyPB (40 nm)/EML (20 nm)/TmPyPB (40 nm)/LiF(1 nm)/Al(150 nm).

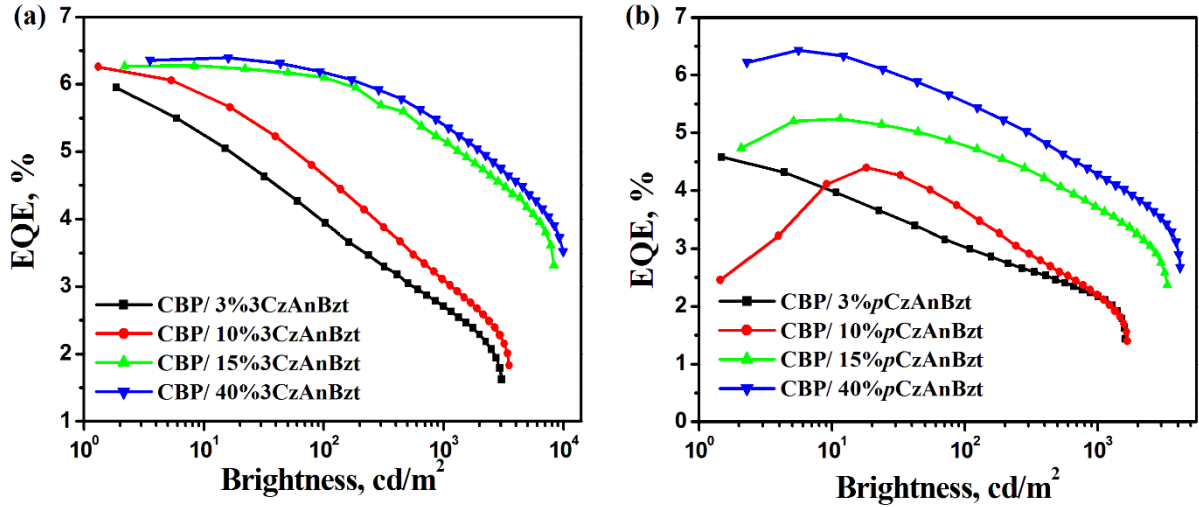


Fig. S13. EQE as a function of brightness of doped devices for **3CzAnBzt** (a) and **pCzAnBzt** (b).

Table S4. Summary of the doped EL performances of OLEDs based on **3CzAnBzt** and **pCzAnBzt**.

| device ^a | V _{on} ^b (V) | L _{max} ^c (cd m ⁻²) | CE _{max} ^d (cd A ⁻¹) | PE _{max} ^e (lm W ⁻¹) | EQE _{max} ^f (%) | λ _{EL} ^g (nm) | CIE ^h (x, y) |
|-------------------------|-------------------------------------|--|---|---|--|--------------------------------------|----------------------------|
| CBP/3% 3CzAnBzt | 3.4 | 3049 | 4.92 | 4.54 | 5.95 | 452 | (0.15, 0.08) |
| CBP/10% 3CzAnBzt | 3.2 | 3507 | 5.77 | 5.66 | 6.25 | 454 | (0.14, 0.09) |
| CBP/15% 3CzAnBzt | 3.0 | 8298 | 6.67 | 6.98 | 6.27 | 458 | (0.14, 0.12) |
| CBP/40% 3CzAnBzt | 3.0 | 9918 | 6.94 | 7.14 | 6.39 | 457 | (0.14, 0.13) |
| CBP/3% pCzAnBzt | 3.6 | 1599 | 2.70 | 2.36 | 4.58 | 450 | (0.15, 0.06) |
| CBP/10% pCzAnBzt | 3.4 | 1659 | 3.01 | 2.58 | 4.39 | 452 | (0.15, 0.07) |
| CBP/15% pCzAnBzt | 3.2 | 3318 | 4.37 | 4.04 | 5.24 | 453 | (0.14, 0.08) |
| CBP/40% pCzAnBzt | 3.2 | 4168 | 5.62 | 5.41 | 6.43 | 453 | (0.14, 0.09) |

^a The uniform device structure: ITO/HAT-CN (15 nm)/TAPC (50 nm)/TCTA (5 nm)/CBP:3%3CzAnBzt or CBP:3%pCzAnBzt (20 nm)/TmPyPB (40 nm)/LiF (1 nm)/Al (150 nm). ^b Voltage at 1 cd m⁻². ^c Maximum luminance. ^d Maximum current efficiency. ^e Maximum power efficiency. ^f Maximum external quantum efficiency. ^g EL emission peak at 6 V. ^h Commission Internationale de l'Éclairage coordinates at 6 V.